Journal Name

ARTICLE

Engineering of bulk and fiber-shaped YAGG:Ce scintillator crystals

O. Sidletskiy[a,*], Ia. Gerasymov[a], D. Kurtsev[a], V. Kononets[a], V. Pedash[a], O. Zelenskaya[a], V. Tarasov[a], A. Gektin[a], B. Grinyov[a], K.Lebbou[b], E. Auffray[c], V. Dormenev[d], A.Borisevich[e], M. Korjik[e]

Received 00th January 20xx,
Accepted 00th January 20xx

DOI: 10.1039/x0xx00000x

www.rsc.org/

Composition-property correlations have been systematically studied in the full concentration range of $Y_3Al_{5-x}Ga_xO_{12}$:Ce (YAGG:Ce) scintillator crystals. The most promising compositions for new high energy physics experiments at colliders have been determined with the light output >200 % relatively to BGO and fast luminescence decay. Codoping with Ca^{2+} provides the decrease of phosphorescence intensity down to 0.2 % after 0.6 µs and shortening of luminescence decay constant to 21 ns. Factors affecting scintillation decay time in YAGG:Ce have been discussed. The crystals show weak transmission loss under γ-irradiation. A feasibility to produce YAGG:Ce fibers by the µ-PD method has been shown.

1. Introduction

Crystals of rare-earth garnets formed by substitution of rare-earth cations and/or Al^{3+}/Ga^{3+} substitutions are now considered to be promising scintillation materials for a number of applications. Ce-doped garnet crystals have cubic spatial symmetry, are not hygroscopic, easy for machining, have emission in the 500-550 nm spectral range matching well the SiPM spectral sensitivity. Recently developed $Gd_3Al_{5-x}Ga_xO_{12}$:Ce (GAGG:Ce) scintillator shows the extremely high light yield up to 58000 phot/MeV among the studied to date oxide scintillators [1,2], and even higher values were reported for Ce-doped $(Gd_2Y_1)Ga_{2.7}Al_{2.3}O_{12}$ crystals [3]. This result is usually attributed to the so-called "bandgap engineering" in garnets, when Ce^{3+} activator emission levels can be positioned in the bandgap by control of the band gap and crystalline field strength at partial cation substitution in the host [4].

$Y_3Al_{5-x}Ga_xO_{12}$:Ce (YAGG:Ce) is another mixed garnet crystal obtained from the ternary Y_2O_3-Al_2O_3-Ga_2O_3 cation system [5,6]. Despite YAGG:Ce overperforms YAG:Ce counterpart by light yield, this scintillator was out of the spotlight due to lower light yield and lower density compared to Lu- and Gd- base multicomponent garnets. A continuous range of solid solutions with the garnet structure from $Y_3Al_5O_{12}$ to $Y_3Ga_5O_{12}$ is formed in YAGG, while in GAGG the garnet phase exists starting from ~20 at% Ga. The structure of Ce^{3+} ion electronic energy levels in YAGG:Ce and GAGG:Ce is similar. YAGG band gap is reduced by 1.0 eV under full substitution of Al by Ga [7]. Ga ions presence in the lattice at the level of 40-60 at.% has positive influence on light yield due to deactivation of shallow traps, which are buried inside the conductance band. However, with increase of the Ga fraction in the compound the conduction band is shrinked, so the lower excited 5d-levels of Ce^{3+} becomes very close to the bottom of the conduction band. In $Y_3Ga_5O_{12}$:Ce this level becomes to be localized within the conductance band. As the result, the room temperature light yield of Ce photo-luminescence, as well as scintillation yield, becomes decreasing due to thermal ionization of electrons from the lowest 5d level of Ce^{3+} at the content of Ga substituting Al more than 60 at.%, and falls down to zero in YGa_3O_{12}:Ce [6].

High energy physics experiments are one of the potential areas of garnet crystals application. As lead tungstate $PbWO_4$ and other scintillators containing heavy elements are severely damaged by high energy hadrons at collider experiments, the upgraded detectors to operate at high luminosity should be based on scintillators consisting of middle heavy atoms [8,9]. While GAGG:Ce is rather dense and contains neutron-sensitive Gd^{3+}, the yttrium garnet seems more relevant for this application. As the 25 ns particle bunch spacing is planned at future colliders (see, for ex. [10]), the target scintillator decay time must be <40 ns. However, the Ce^{3+} radiative decay time in garnets emitting at 550-600 nm is never faster than 50-60 ns, because of the fundamental limitation of luminescence lifetime $\tau \sim \lambda^3$ (λ – emission wavelength) [11]. Scintillation decay time is even longer keeping in mind the time needed for carrier transport to the luminescence center. For instance, the fast component of scintillation decay time in YAG:Ce ranges from 55 to 120 ns [12,13] besides the long components with the decay times within hundreds of nanoseconds. Therefore, 40 ns decay time is not achievable in Ce^{3+}-doped garnets, unless some luminescence quenching process is introduced. Recently, it was shown that the luminescence decay kinetics in garnets may be shortened by the codoping with divalent cations, such as Ca^{2+} and Mg^{2+} (see, for ex. [14-16]). As the divalent ions codoping promotes

[a] Institute for Scintillation Materials NAS of Ukraine, 60 Nauky ave., 61001 Kharkiv, Ukraine
[b] Institute Lumière Matière, UMR5306 CNRS, Universite de Lyon 1, 69622 Villeurbanne Cedex, France
[c] European Organization for Nuclear Research, Geneva 23, Switzerland
[d] Justus-Liebig-Universität Gießen II. Physikalisches Institut, 16 Heinrich-Buff-Ring, Gießen, Germany
[e] Research Institute for Nuclear Problems of Belarus State University,220030, 11Bobruiskaya str, Minsk, Belarus
* Corresponding author

Please do not adjust margins

simultaneous creation of hole defects and deep electronic traps and transformation of some fraction of Ce^{3+} into the tetravalent state, the strong competition with shallow traps for capture electrons from the conductance band occurs what thereby promotes the faster scintillation decay. However, an appearance of the new hole defects and deep electronic traps due to the codoping with the divalent cations also introduces some luminescence quenching that reduces scintillation light yield.

In this work we present an another approach to decrease a scintillation decay time in garnets based on combination of the energy structure engineering in YAGG:Ce by Al/Ga substitution and divalent cation codoping. Overall there are three main factors expected to promote the decay time decrease with Ga addition in YAGG:Ce.

First, weakening of the crystalline field and smaller Ce^{3+} d^1-configuration levels splitting [17] results in luminescence band blue-shift by ~50 nm [6] favoring decay time shortening [11]. Second, the band gap decrease by 1.0 eV at full Al^{3+} substitution with Ga^{3+} [6] diminishes the energy gap between Ce^{3+} $5d_1$ radiating state and the bottom of conduction band and promotes thermal ionization of electrons to the conduction band from this level. The decrease of the room temperature luminescence lifetime down to ~20 ns at intracenter Ce^{3+} excitation at 337 nm with Al/Ga substitution was reported on YAGG:Ce polycrystalline sample with 75 at% Ga [17], and a similar effect of the increase of relative content of the fastest component in the scintillation response with Ga addition was noted in the $Y_2Gd(Al,Ga)O_{12}$:Ce solid solution[18]. Third, codoping with Ca^{2+} by the analogy with other complex oxides (the examples will be discussed hereafter) simplifies the carrier transport to cerium activator.

Therefore, this paper represents the analysis of scintillation parameters of YAGG:Ce single crystals under the full range of Al/Ga substitution and Ca^{2+} codoping with the focus on possibilities of decay time shortening.

2. Experimental

The part of samples was cut from crystals grown in the previous study [6]. These crystals were fabricated from melts with Ga content 0, 20, 40, 60, 100 at.%. As the work is focused on search for compositions with shorter luminescence decay times, additionally the crystals with Ga content 75% and 85% were grown by the Czochralski method by the same procedure. The Ca-codoped crystal with Ga content 75 % was grown from the melt containing 0.15 at% Ca. The samples with 10x10x2 mm dimensions and polished 10x10 faces were cut for scintillation measurements.

Light output and energy resolution under γ-rays was measured with 662 keV ^{137}Cs γ-source and a R1307 Hamamatsu PMT ran at 800 V HV with linear dynode voltage divider. PMT output was connected to the charge-sensitive preamplifier BUS 2-94, BUI-3K linear amplifier, and AMA-03F multichannel analyzer. Signal from preamplifier was shaped by custom shaping amplifier with the shaping times of 2 μs and 8 μs. During measurements the crystals were coupled to the PMT entrance window using silicon optical compound Visilox V-788. In order to collect the whole scintillation light the crystal together with open part of PMT photocathode were covered by 3 layers of Teflon tape. Energy resolution was determined by approximation of 662 KeV peaks by the Gaussian function. Instrumental error of light output and energy resolution determinations does not exceed 5%. Luminescence decay times under 662 keV ^{137}Cs γ-rays excitation were measured using 9814QB PMT from ET Enterprises. Signal from PMT anode was fed to 50 Ohm terminated input of Rigol DS6064 digital oscilloscope. Decay curves were calculated by averaging several hundreds of raw pulses with energies close to the position of full absorption peak. Moreover, light yield and scintillation decay times under ^{22}Na 511 keV γ-rays were measured with laboratory bench on a base of XP2020PMT with a custom made start-stop spectrometer based on two XP2020 PMTs.

Absorption spectra of crystals were measured with a Specord Analytik Jena 40 spectrometer. Change of the optical transmission of samples with different Ga content under γ-rays irradiation was studied using ^{60}Co source with dose rate around 1.5 Gy/minute, and the total absorbed dose is 100 Gy. Transmission spectra before and after the irradiation were measured using a Varian spectrophotometer.

All the measurements were made at room temperature.

3. Results and discussion

3.1 Growth of YAGG:Ce bulk crystals

$Y_3(Al_{1-x}Ga_x)_5O_{12}$:Ce (YAGG) crystals with the Ga content 75 and 85 %, and the 22-25 mm diameter and 50-100 mm length were grown on a YAG seed with [100] orientation by the Czochralski method using Ir crucibles with the 40 mm diameter and 30 mm height.

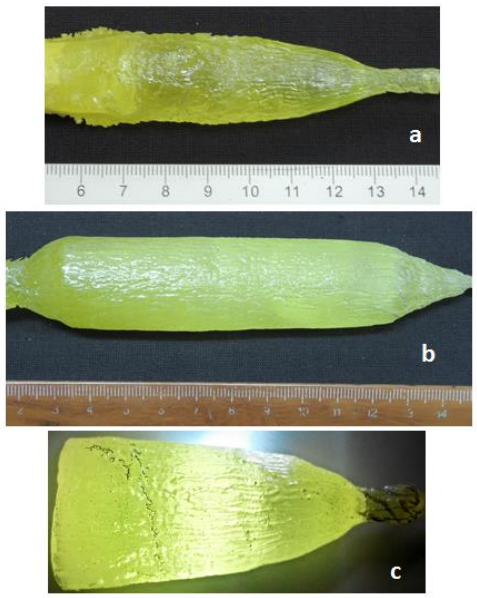

Fig. 1. As grown YAGG:Ce crystals: a – YAGG:Ce (75 at. % Ga); b – YAGG:Ce,Ca (75 at. % Ga); c - YAGG:Ce (85 at. % Ga).

Growth atmosphere was Ar+1%O_2. Oxygen was added to atmosphere to inhibit melt evaporation. CeO_2 concentration in melt was maintained at 1 mol.% level. All the crystals were exposed to post growth annealing in O_2-containing atmosphere at 1300 ºC. Prior study of cation distribution in YAGG:Ce [6] showed that Ga segregation coefficient is around 1, and k_{eff}(Ce) smoothly increases from 0.07 in YAG to 0.17 in YGG due to lattice loosening by the introduction of larger Ga^{3+} cation. According to these results, the k_{eff}(Ce) in YAGG:Ce at Ga content 75-85 % is expected to be around 0.15.

3.2. Light output and energy resolution

It was shown that light yield YAGG:Ce reaches its maximum at Al/Ga ratio 1:1 and reaches 0 at full substitution of Al with Ga[6,7]. This trend was confirmed in this work with a larger amount of intermediate compositions (Table 1). The maximal relative light output (not accounting for matching between the emission and PMT sensitivity bands) was registered at 75% Ga. At further Ga addition the light output sharply falls due to the strong thermal quenching – the very low light output was observed for the sample with 85 % Ga concentration, while no scintillation signal was detected in YGG:Ce. Ca^{2+} codoping diminishes the light yield in the 75 % Ga samples to the BGO level. The values and trends are similar for 2 µs and 8 µs shaping times pointing the inessential contribution of slow luminescence components.

The energy resolution in YAGG:Ce is within 17-19 % at 662 keV, which is significantly worse compared to the best values of ~5 – 7 % for PMT readout reported for other multicomponent garnets [19,20] .

Table 1. Scintillation parameters of YAGG:Ce crystals irradiated with ^{137}Cs 662 keV γ-rays.

Compo-sition (%Ga)	Light output (BGO=100 %) for shaping times		Energy resolution, % at 662 keV for 2 µs shaping time	Main decay time, ns	Afterglow, % (after 0.6µs)
	2 µs	8 µs			
0	51	56	14.9	135	7.9
20	ND	70	ND	105	7.7
40	85	108	17.6	92	8.5
60	150	148	19.2	28	1.6
75	234	232	18.1	37	1.4
75 (+Ca)	99	99	22.9	21	0.2
85	15	15	18.0	glow	~60
100	0	0	-	-	-

The study of the sample with 75 % Ga under ^{22}Na 511 keV γ-rays (Fig. 2) gives the light yield about 20 % relatively to the reference GAGG:Ce sample with the light yield about 50000 phot/MeV.

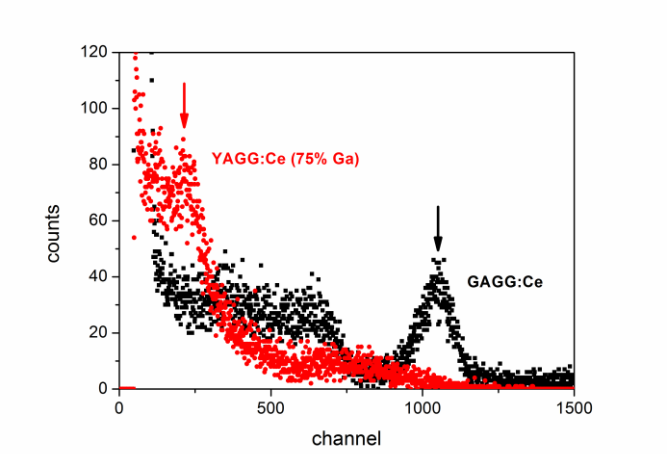

Fig. 2. Amplitude spectra of YAGG:Ce (75% Ga) crystal under ^{22}Na γ-excitation in comparison with GAGG:Ce. Light yield of YAGG:Ce crystal was determined relatively to GAGG:Ce crystal by comparison of photopeaks of 511 keV γ-quanta. The compared 511 keV photopeaks are marked with arrows.

3.3. Decay time and phosphorescence

By scintillation decay behavior the studied crystals can be separated into three distinct groups (Fig. 3). The first group of crystals with the main decay times around 100 ns (fitting by one exponent) comprise YAG:Ce, as well as YAGG:Ce with 20 and 40% Ga. The second group of crystals with fast decay is represented by YAGG:Ce with the Ga content 60 and 75%. The shortest main decay time component of 21 ns is achieved in 75% Ga crystals codoped with Ca^{2+}. The luminescence decay times in the third group of crystals represented by YAGG:Ce crystal with 85% Ga are too long to be exactly determined from the measured curves, while no luminescence was registered in YGG:Ce.

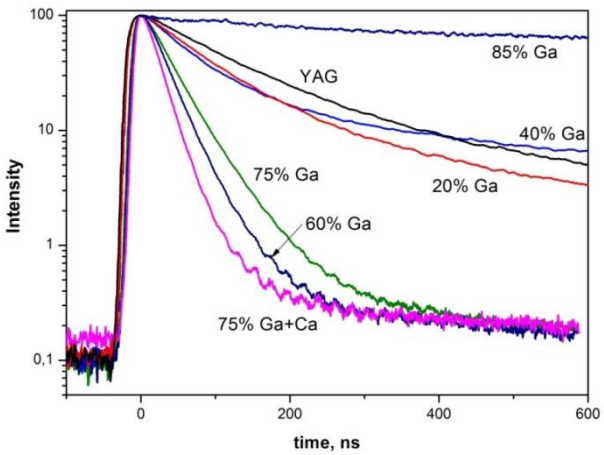

Fig. 3. Scintillation decay in YAGG:Ce crystals under 662 keV ^{137}Cs excitation.

The decay time sharply drops between the samples with 40 and 60% Ga, though the common trend of decay time decrease with Ga concentration is clear. Recently [21], it was shown that Ga^{3+}

preferably occupies the tetrahedral sites in YAGG (though larger Ga^{3+} atoms was supposed to occupy first the larger octahedral sites). The interval between 40 and 60 % of Ga corresponds to the situation when the number of Ga atoms exceeds the number of Al atoms and Al^{3+}/Ga^{3+} substitution into octahedral sites starts. Likely, the Ga introduction into the octahedral sites strongly affects the Ce^{3+} luminescence center geometry and its luminescence characteristics.

The scintillation decay was measured under ^{22}Na (511 KeV) excitation too (Fig. 4). Fitting by the two exponents gives the fast component decay time of 28 ns with the contribution of 96 %, and the slow component of 89 ns with the contribution of 4 %. The data obtained under different energies in different laboratories are consistent with each other.

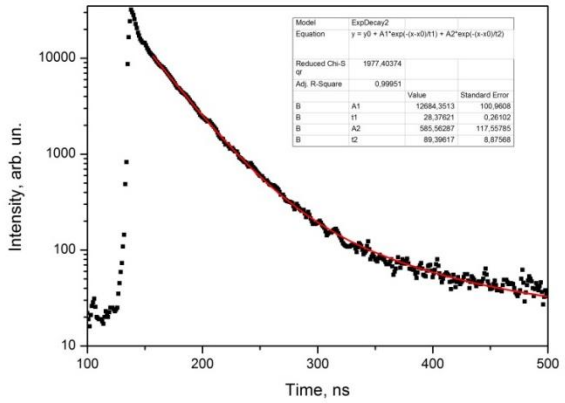

Fig. 4. Scintillation decay of YAGG:Ce (75% Ga) crystal under ^{22}Na (511 keV) γ-excitation.

3.4. Change of the optical transmission under γ-irradiation

The samples with different Ga content were irradiatied with γ-rays, dose 100 Gy. The transmission was measured before and after the irradiation (Fig. 5). The larger impact of irradiation is seen for YAG:Ce and YAGG:Ce (40% Ga) samples, while no visible deterioration is observed in the samples with higher Ga content. The major changes in transmission are observed in the UV-range while the irradiation very weakly affects the transmission in the range of Ce^{3+} luminescence at 500-550 nm. It points a good tolerance to irradiation with γ-quanta. As YAGG:Ce does not contain heavy atoms, a good radiation hardness to a hadron irradiation is expected. The irradiation by high energy protons is under way.

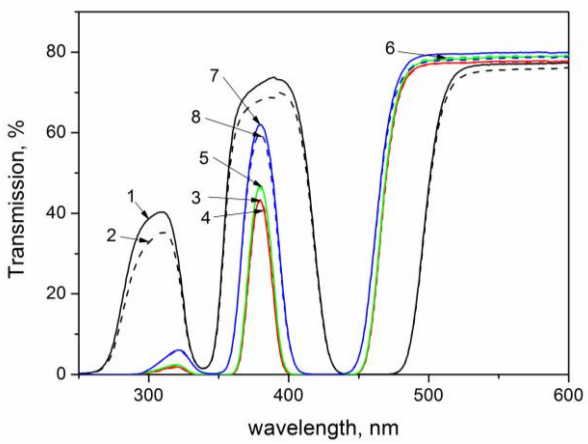

Fig. 5. Impact of irradiation with γ-rays, dose = 100 Gy on transmission of YAGG:Ce crystals with different Ga content: 1 – YAG:Ce (before irradiation), 2 – YAG:Ce (after irradiation), 3 – YAGG:Ce 20%Ga (before irradiation), 4 - YAGG:Ce 20%Ga (after irradiation), 5 - YAGG:Ce 60%Ga (before irradiation), 6 - YAGG:Ce 60%Ga (after irradiation), 7 - YAGG:Ce 75%Ga (before irradiation), YAGG:Ce 75%Ga (after irradiation).

3.5. Search for the optimal YAGG:Ce composition

Following the data summarized in Table 1, Ga addition in YAGG:Ce up to 75 % has the positive impact on both light yield and scintillation decay time. The light yield trend with Al/Ga substitution is in agreement with an empirical prediction of light yield improvement dependence on ionic radii ratio of substituted atoms in mixed crystals [28]. The light yield improvement may be due to deactivation of electron shallow traps, which levels are situated in YAG:Ce under the conductance band. Addition of > 75 % Ga shifts the Ce $5d_1$ level very close to the edge of the conductance band and completely kills the Ce^{3+} 5d-4f radiative transitions (see Fig. 6) in YGG:Ce. The high Ga content leads to the ionization of electrons from 5d Ce^{3+} levels into the conductance band and calls strong phosphorescence (afterglow), as observed with the 85 % Ga sample.

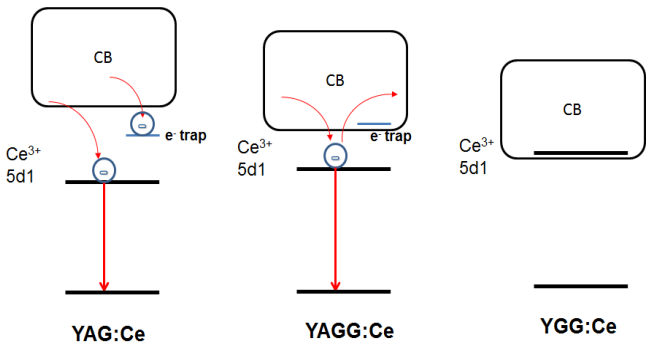

Fig. 6. Band gap engineering in YAG:Ce – YGG:Ce system.

Doping with Ca^{2+} provided the reduction of the phosphorescence down to 0.2 % after 0.6 μs. Therefore, divalent ion codoping calls a strong competition between shallow electron traps on one hand,

and deep electron traps and Ce^{4+} on the other hand, resulting in suppression of the phosphorescence. Some light output decrease with Ca^{2+} codoping indicates also a luminescence quenching process. Therefore, the Ga content 60 – 75 % in YAGG is the optimal composition range from the point of brightness and fast luminescence decay.

A clear fingerprint of Ce^{4+} - O^{2-} complex charge transfer absorption in Ca^{2+}-codoped crystal is observed around 300 nm (Fig. 7) in agreement with numerous papers on divalent cation copoding of Ce-doped complex oxides – see for ex., the references related to orthosilicates [22,23], garnets [24,25] and perovskites [26]. Ca^{2+} induces cerium transfer into the tetravalent state thus promoting the faster scintillation decay. Worth to note that Ga^{3+} doping itself may increase the fraction of Ce^{4+} in multicomponent garnets [27].

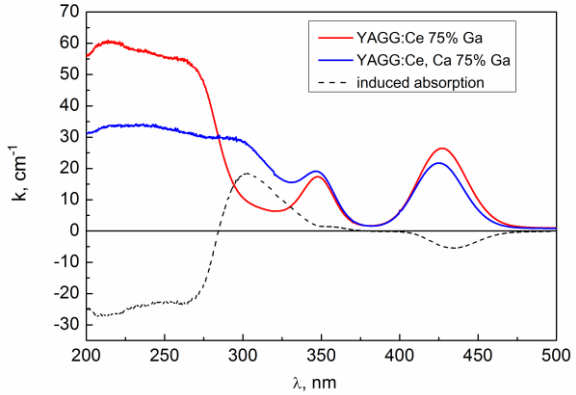

Fig. 7. Absorption spectra of YAGG:Ce (75% Ga) and YAGG:Ce,Ca (75% Ga) crystals, and the induced absorption spectrum.

3.6. Growth of YGG and YAGG:Ce fibers by the micro-PD method

As fiber-shaped scintillation detectors is one of the possible designs of new high granularity calorimeters in high-energy physics, we attempted to grow YAGG:Ce fibers by the micro-PD method. The fiber growth process was similar to the LuAG and LuAG:Ce growth procedure described in [29]. Ground parts of YGG and YAG:Ce crystals fabricated in ISMA by the Czochralski method were used as raw materials. Fibers with the 2 mm diameter were pulled with the 0.3 - 0.5 mm/min rates on the seed with the crystallographic orientation [111].

YGG fiber by its quality can be distinguished into 3 parts (Fig. 8):
(i) Lengths 0→1.6 cm. Numerous cracks in the beginning were formed, probably, due to the different cell parameters [6] of YAG and YGG.
(ii) Lengths 1.6→3.2 cm. The fibers became darker. The surface is mat, however, there are almost no cracks inside, because the growth process was stabilized and mechanical stress due to the lattice mismatch between the seed and the fiber was reduced.
(iii) Lengths 3.2→4.5 cm. The fiber became thinner and slightly curved. This part of the fiber is surprisingly transparent but full of long heavy cracks. Evidently, this part of fiber was grown from non-stoichiometric melt with lack of Ga due to its evaporation. The Ga_2O_3 layer was deposited on the inner side of the crystallizer.

The YAGG:Ce fiber (75 at% Ga, 150 ppm of Ce) was opaque and completely polycrystalline. Ga deposited on the crystallizer in less quantity compared to the YGG growth. The YAGG:Ce fiber consists of the fragile opaque layer surrounding the strong core part, similar to that we observed with LGSO:Ce fibers [30]. We attributed these complications to (i) radial segregation of larger cations (Ga^{3+} in the case of YAGG) to the periphery of fibers, and (ii) melt and crystal non-stoichiometry due to Ga oxide evaporation from the melt.

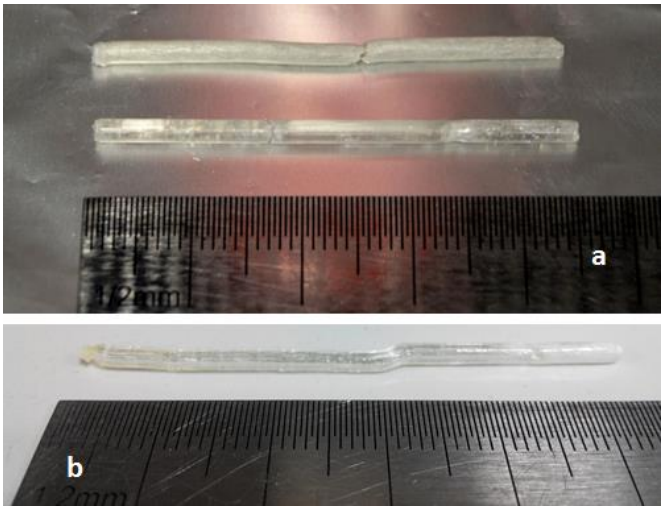

Fig. 8. Photos of as-grown fibers: (a) YGG, (b) YAGG:Ce obtained after optimization of growth conditions. The beginnings of fibers are on the left.

As the 1st factor cannot be excluded from the growth process, the second one was diminished by addition of melt of 3% excess of Ga to compensate its losses by evaporation. Though the shape of the new fiber with the 5 cm length was still not good, the fiber was crackless and transparent besides the final part of ~ 1 cm length. It shows that control of Ga excess is a way to obtain crackless YAGG:Ce fibers.

All the fibers were not straight, evidently because meniscus overcooling at some stages and contact of fiber crystallization interface with Ir capillary. Therefore, thermal conditions of fiber pulling should be further optimized.

Conclusions

YAGG:Ce is a promising bright, fast and radiation hard scintillator for high energy physics experiments. The optimal combination of scintillation parameters: light output up to 230 % relatively to BGO, 20-40 ns decay times were achieved at Ga concentrations 60 - 75 at%. The phosphorescence intensity in YAGG:Ce can be suppressed down to 0.2 % (after 0.6 μs) by Ca^{2+} codoping. The registered decay time reduction is due to (i) blue-shift of luminescence spectrum, and (ii) thermal ionization of carriers from the lowest Ce^{3+} excited level at Ga^{3+} addition. By the analogy to other Ce-doped complex oxide scintillators, (iii) cerium transfer into tetravalent state at Ca^{2+}-codoping should suppress carrier trapping and simplify the carrier transport to the luminescence center. Despite the problem of

significant Ga losses by melt evaporation, a feasibility to grow transparent YAGG:Ce fibers without cracks by the micro-PD method is shown.

Acknowledgements

The work is partially supported by the Marie Skłodowska-Curie Research, Innovation Staff Exchange Project H2020-MSCA-RISE-2014 no.644260 "INTELUM". The Ukrainian and French teams also acknowledge the support from Ukrainian-French PICS project between CNRS (Project no.6598) and National Academy of Sciences of Ukraine (ProjectF1-2016).

Authors acknowledge Dr. S. Vasiukov (ISMA NAS of Ukraine) for providing optical absorption measurements.

Notes and references

1 K. Kamada, S. Kurosawa, P. Prusa, M. Nikl, V. Kochurikin, T. Endo, K. Rsutumi, H. Sato, Y. Yokota, K. Sugiyama, A. Yoshikawa, *Opt. Mater.*, 2014, **36**, 1942.
2 M. Tyagi, A. K. Singh, S. G. Singh, D. G. Desai, G. D. Patra, S. Sen, and S. C. Gadkari, *Phys. Status Solidi RRL*, 2015, **9**, 530.
3 C. Wang, Y. Wu, D. Ding, H. Li, X. Chen, J. Shi, G. Ren, *Nucl. Instrum. Methods Phys. Res., Sect. A,* 2016, 820, 8.
4 M. Fasoli, A. Vedda, M. Nikl, C. Jiang, B.P. Uberuaga, D.A. Andersson, K.J. McClellan, C.R. Stanek, *Phys. Rev. B*, 2011, **84**, 081102(R).
5 K Kamada, T Yanagida, J Pejchal, M Nikl, T Endo, K Tsutumi, Y Fujimoto, A Fukabori and A Yoshikawa, *J. Phys. D: Appl. Phys*., 2011, **44**, 505104.
6 O. Sidletskiy, V. Kononets, K. Lebbou, S. Neicheva, O. Voloshina, V. Bondar, V. Baumer, K. Belikov, A. Gektin, B. Grinyov, *Mater. Res. Bull*., 2012, **47**, 3249.
7 Yu. Zorenko, T. Zorenko, P. Malinowski, O. Sidletskiy, S. Neicheva, *J. Lumin*., 2014, **156**, 102.
8 E. Auffray, A. Barysevich, A. Fedorov, M. Korjik, M. Koschan, M. Lucchini, V. Mechinski, C.L. Melcher, A. Voitovich., *Nucl. Instrum. Methods Phys. Res., Sect. A*, 2013, **721**, 76.
9 E. Auffray, A. Borisevitch, A. Gektin, Ia. Gerasymov, M. Korjik, D. Kozlov, D. Kurtsev, V. Mechinsky, O. Sidletskiy, R. Zoueyski, *Nuclear Nucl. Instrum. Methods Phys. Res., Sect. A*, **783**, 117.
10 LHC Detectors Upgrade, Technical Design Report, Vol. 1. Protons. CERN–ACC–2014-0337, 15 December 2014 (https://cds.cern.ch/record/1976692/files/CERN-ACC-2014-0337.pdf).
11 P Dorenbos, *Nuclear Nucl. Instrum. Methods Phys. Res., Sect. A*, 2002, **486**, 208.
12 Scintillation Properties. S. Derenzo, M. Boswell, M. Weber, and K. Brennan (http://scintillator.lbl.gov/).
13 M. Nikl, A. Yoshikawa, K. Kamada, K. Nejezchleb, C.R. Stanek, J.A. Mares, K. Blazek, *Prog. Cryst. Growth Charact*, 2013, **59**, 47.
14 K. Kamada, M. Nikl , S. Kurosawa, A. Beitlerova , A. Nagura, Y. Shoji, J. Pejchal, Y. Ohashi , Y. Yokota, A. Yoshikawa, *Opt. Mater.*, 2015, **41**, 63.
15 Yuntao Wu, Fang Meng, Qi Li, Merry Koschan, and Charles L. Melcher, *Phys. Rev. Applied*, 2014, **2**, 044009.
16 A. Nagura, K. Kamada, M. Nikl, S. Kurosawa, J. Pejchal, Y. Yokota, Y. Ohashi and A. Yoshikawa, *Jpn. J. Appl. Phys., 2015,* **54,** 04DH17.
17 Rachael A. Hansel, S. W. Allison, and D. G. Walker, *Appl. Phys. Lett.*, 2009, **95**, 114102.
18 W. Chewpraditkul, D. Panek, P. Prusa, W. Chewpraditkul, Ch. Wanarak, N. Pattanaboonmee, V. Babin, K. Bartosiewicz, K. Kamada, A. Yoshikawa, and M. Nikl, *J. Appl. Phys*., 2014, **116**, 083505.
19 Y. Wu, Z. Luo, H. Jiang, F. Meng, M. Koschan, Ch.L. Melcher, *Nucl. Instrum. Methods Phys. Res., Sect. A,* 2015, **780**, 45.
20 A. Giaz, G. Hull, V. Fossati, N. Cherepy, F. Camera, N. Blasi, S. Brambilla, S. Coelli, B. Million, S. Riboldi, *Nucl. Instrum. Methods Phys. Res., Sect. A*, 2015, **804**, 212.
21 V. Laguta, Yu. Zorenko, Yu. Zagorodny, O. Sidletskiy, P. Bilski, A. Twardak, M.Nikl, *J. Phys. Chem. C*, 2016, **120**, 2016, 24400.
22 S. Blahuta, A. Bessiere, B. Viana, P. Dorenbos, V. Ouspenski, *IEEE Trans. Nucl. Sci*., 2013, 60(4), 3134.
23 W. Chewpraditkul, Ch. Waranak, T. Szcxesniak, M. Miszynski, V. Jary, A. Beirlerova, M. Nikl, *Opt. Mater*., 2013, **35**, 1679.
24 M. Tyagi, F. Meng, M. Koschan, S. Donnald, H. Rothfuss and Ch. Melcher, *J. Phys. D: Appl. Phys*., 2013, **46**, 475302.
25 M. Nikl, K. Kamada, V. Babin, J. Pejchal, K. Pilarova, E. Mihokova, A. Beitlerova, K. Bartosiewicz, S. Kurosawa, and A. Yoshikawa, *Cryst. Growth Des.*, 2014, **14**, 4827.
26 F. Moretti, K. Hovhannesyan, M. Derdzyan, G. Bizarri, E. Bourret, A. Petrosyan, and C. Dujardin, *ChemPhysChem*, 2016, DOI: 10.1002/cphc.201601190.
27 Y. Wu, J. Luo, M. Nikl, and G. Ren, *APL Materials*, 2014, **2** 012101.
28 O. Sidletskiy, A. Gektin, and A. Belsky, *Phys. Status Solidi A. 2014,* **211**, 2384.
29 V. Kononets, E.Auffray, C.Dujardin, S.Gridin, F.Moretti, G.Patton, K.Pauwels, O. Sidletskiy, X.Xu, K.Lebbou, *J. Cryst. Growth*, 2016, **435**, 31.
30 V. Kononets, O. Benamara, G. Patton, C. Dujardin, S. Gridin, A. Belsky, D. Dobrovolskas, A. Vaitkevičius, G. Tamulaitis, V. Baumer, K. Belikov, O. Sidletskiy, K. Lebbou, *J. Cryst. Growth,* 2015, **412**, 95.

